HETEROCYCLES, Vol. 106, No. 8, 2023, pp. 1385 - 1396. © 2023 The Japan Institute of Heterocyclic Chemistry
Received, 5th June, 2023, Accepted, 10th July, 2023, Published online, 11th July, 2023
DOI: 10.3987/COM-23-14872

THEORETICAL INVESTIGATION OF Cp*Co(III)-MEDIATED REGIOSELECTIVE [4 + 2]-ANNULATION OF *N*-CHLOROBENZAMIDE WITH VINYL ACETATE FOR THE SYNTHESIS OF ISOQUINOLONE

Nan Lu,* Chengxia Miao, and Xiaozheng Lan

The affiliations are desired to be typewritten in English. College of Chemistry and Material Science, Shandong Agricultural University, Taian City 271018, Shandong Prov., P.R. China; E-mail: lun@sdau.edu.cn

Abstract – The mechanism is investigated for regioselective [4 + 2]-annulation of *N*-chlorobenzamide catalyzed by Cp*Co(III). The $CoCp^*(OAc)_2$-mediated *ortho*-cobaltation via acetate-aided N-H and C−H deprotonation furnishes a five-membered intermediate, which is coordinative inserted into alkene by giving seven-membered cobaltacycle. The reductive elimination and oxidative addition of CoCp*(I) species afford six-membered ring. The recovery of CoCp*(III) is assisted by one AcOH for vinyl acetate with OAc group available to cleavage as one ligand. Two OAc ligands are both supplied by AcOH for vinyl ketone with COMe group difficult to break. The acetate-assisted tautomerization produces isoquinolin-1(2*H*)-one. The 3-acetylisoquinolin-1(2*H*)-one is given by dehydrooxidation. The promotion of Cp*Co(III) lies in the barrier decrease of most steps especially N-H and C−H deprotonation. AcOH functions in the protonation of Cl, N and as sources of acetate ligands for the recovery of CoCp*(III). These results are supported by Multiwfn analysis on FMO of specific TSs and MBO value of vital bonding, breaking.

As the most common heterocyclic skeletons, isoquinolones are present in various natural products and pharmaceuticals. Their derivatives exhibit broad medicinal properties, including antitumor, antiobesity, antiviral, and other effects.[1,2] Hence, the development of practical and efficient synthetic protocol for the construction of isoquinolones and their analogues is a continuous need of synthetic chemists. Among numerous synthetic methods available in organic synthesis, transition-metal-catalyzed annulation of substituted arenes with π-components has gained considerable attention due to its step- and cost-effective manner.[3-5] In recent years, some novel protocols have constantly emerged such as Rh(III)-catalyzed C−H

activation/annulation affording diverse peptide-isoquinolone conjugates, Ru(II)-catalyzed C−H/N−H bond functionalization of *N*-chlorobenzamides with 1,3-diynes via regioselective [4 + 2]-annulation under redox-neutral conditions at room temperature, Rh(III)-catalyzed oxazolinyl-directed C−H activation and tandem annulation from 2-oxazolines, iodonium ylides, and carboxylic acids, Rh(III)-catalyzed [4 + 2]-annulation of benzamide with coupling reagent methyl 2-chloroacrylate, and $LiN(SiMe_3)_2$/KO^{t}Bu-promoted formal [4 + 2]-cycloaddition of 2-methylaryl aldehydes and nitriles.[6-10]

The alkynes, vinyl acetates, azabenzonorbornadienes, and vinyl formamides are usually employed as π-components to synthesize isoquinolone derivatives. The rhodium, palladium, iridium, and ruthenium are commonly present to accomplish the site-selective C−H annulation of substituted arenes with alkenes.[11-14] However, the less abundance of these noble transition-metal complexes on earth and high cost restrain the development of this methodology in future. Therefore, notable prosperity has been focused on the improvement of protocols using 3d-metal complexes for the C−H functionalization of arenes. In past two decades, Prakash has already considered less expensive cobalt and summarized Co-catalyzed directing group assisted C−H activation/cyclization.[15] Muniraj reported cobalt-catalyzed regioselective [4+2]-annulation/lactonization of benzamides with 4-hydroxy-2-alkynoates under aerobic conditions.[16] Dey realized Co-catalyzed sp^2-C−H activation and [4 + 2]-annulation with 1,3-diynes assisted by traceless bidentate directing group.[17] Then he synthesized indane derivatives using Co-catalyzed diastereoselective [3 + 2]-annulation of allenes.[18] In particular, Rogge analyzed the reactivity-controlling factors in carboxylate-assisted C−H activation of arenes under 3d and 4d transition metal catalysis.[19] Nandy provided valuable insight into why conventional design rules for C−H activation fail for open-shell transition-metal catalysts.[20]

As early as in 2019, Chen disclosed rhodium(III)-catalyzed oxidative cyclization of benzoic acids with vinyl formamide yet requiring external oxidants.[21] Therefore, searching for a redox-neutral manner for the preparation of valuable isoquinolones became a hot topic. Of special interest to us is Cp*Co(III)-catalyzed annulation of arenes with various alkenes including acrylates, styrenes, unactivated alkenes, and vinyl acetates.[22-24] A new breakthrough was Murugan's CoCp*(III)-catalyzed [4 + 2]-annulation of *N*-chlorobenzamides with vinyl acetate/vinyl ketones.[25] Nevertheless, how the active catalyst was regenerated was still unknown. Although some speculation was supported by deuterium labeling, there is no report about detailed mechanistic study involving ortho C−H bond of *N*-chlorobenzamide especially the key role of N−Cl bond as an internal oxidant. What's the origin of regioselectivivity for $CoCp^*(OAc)_2$-aided *ortho*-cobaltation in this [4 + 2]-annulation? How the transition between acetic acid and acetate influence the recovery of Cp*Co(III)? Why different final products isoquinolin-1(2*H*)-one and 3-acetylisoquinolin-1(2*H*)-one were produced when applying vinyl acetate and vinyl ketone? To solve these mechanic problems in experiment, an in-depth theoretical study was

necessary for this effective method suitable for electronically diverse *N*-chlorobenzamides. The density functional theory (DFT) method was employed focusing on the promotion of Cp*Co(III).

Based on the experimental research previously,[23-25] the mechanism was explored for Cp*Co(III)-mediated regioselective [4 + 2]-annulation of *N*-chlorobenzamide **1** with vinyl acetate **2**a, vinyl ketone **2**b leading to isoquinolin-1(2*H*)-one **3**a, 3-acetylisoquinolin-1(2*H*)-one **3**b (Scheme 1). Initially, the $CoCp^*(OAc)_2$ **A**-catalyzed *ortho*-cobaltation via acetate-aided N-H and C−H deprotonation furnishes a five-membered intermediate **B**. Subsequently, alkene **2**a/**2**b (R=OAc/COMe) undergoes coordinative insertion into **B**, giving seven-membered cobaltacycle intermediate **D**/**G**, from which the reductive elimination and oxidative addition of CoCp*(I) species afford six-membered intermediate **E**/**H** with N−Cl bond. Next is the recovery of active catalyst CoCp*(III) assisted by AcOH and generation of last intermediates **F**/**I**. With OAc group available to be cleavage, the substrate ratio is 1:1 for **E**. While two molecules of AcOH are required for **H** with COMe group uncoordinated to Co also difficult to break. Finally, the basic acetate-assisted tautomerization of **F** leads to product **3**a and the dehydrooxidation of **I** yields **3**b. The optimized structures of TSs and intermediates in Scheme 2 are listed by Figure 1 and Supplementary Figure S1, respectively. Table 1 and Supplementary Table S1, Table S2 show the activation energy of all reactions and the relative energies of all stationary points. The Gibbs free energies in DCE solution phase are discussed here to be in accordance with experiment.

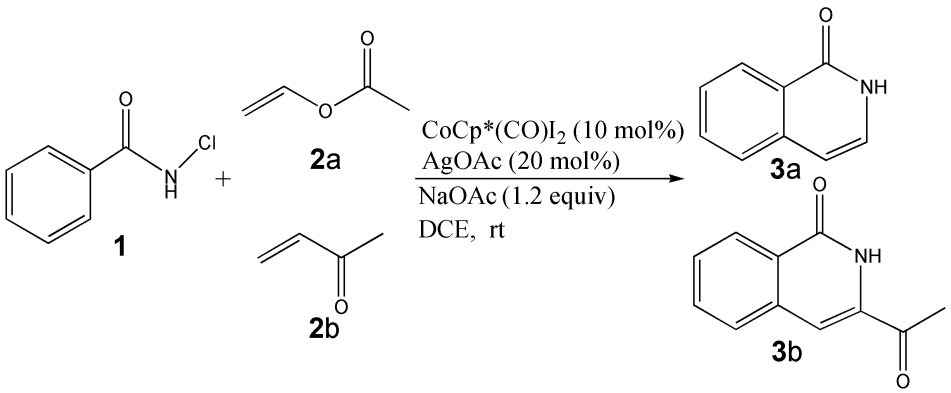

Scheme 1. Cp*Co(III)-mediated regioselective [4 + 2]-annulation of *N*-chlorobenzamide **1** with vinyl acetate **2**a, vinyl ketone **2**b leading to isoquinolin-1(2*H*)-one **3**a, 3-acetylisoquinolin-1(2*H*)-one **3**b.

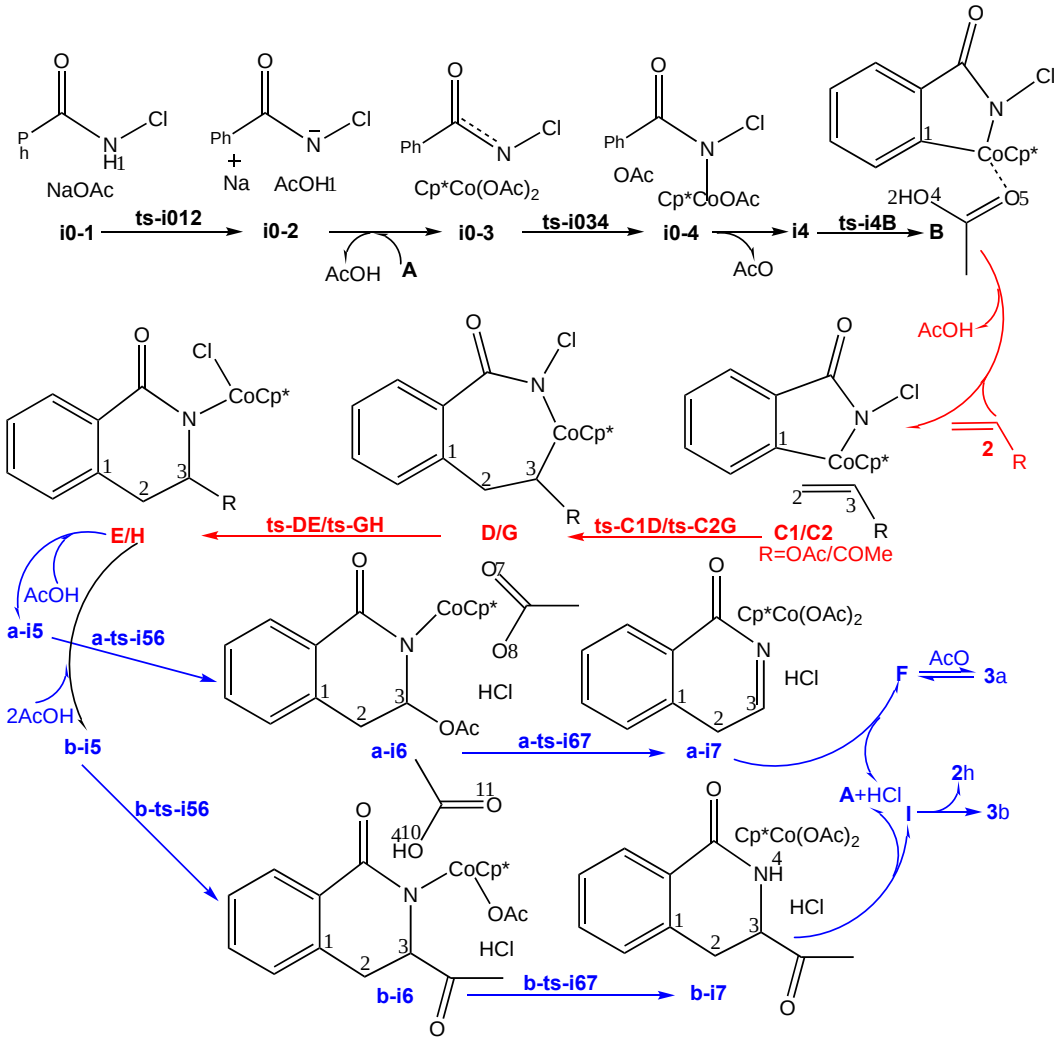

Scheme 2. Proposed reaction mechanism of Cp*Co(III)-mediated regioselective [4 + 2]-annulation of **1** with **2**a, **2**b yielding **3**a, **3**b. TS is named according to the two intermediates it connects.

Table 1. The energy level and activation energy in solvent (in kcal mol^{-1}) of all reactions

TS	$\Delta G^{\neq}_{sol}$	$\Delta\Delta G^{\neq}_{sol}$
ts-i12	26.1	26.1
ts-i23	36.7	21.3
ts-i4B	18.9	18.9
ts-i012	1.9	1.9
ts-i034	21.7	21.7
ts-C1D	9.7	9.7
ts-DE	13.1	24.8
a-ts-i56	20.0	20.0
a-ts-i67	25.8	15.4
ts-i89	6.8	6.8

ts-i910	-31.2	8.2
ts-C2G	5.8	5.8
ts-GH	12.1	28.4
b-ts-i56	40.1	40.1
b-ts-i67	18.0	2.9

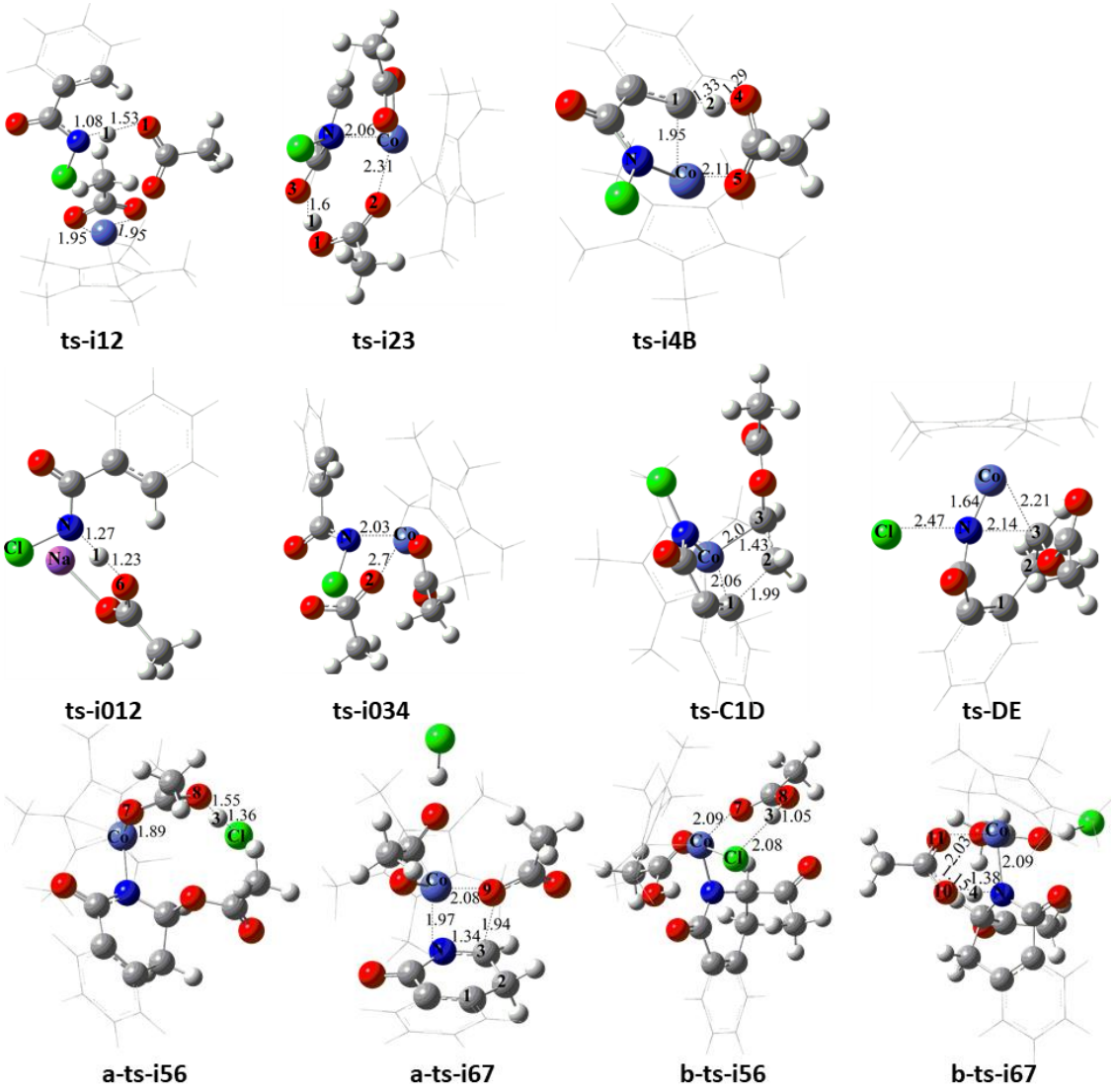

Figure 1. Optimized structure of transition states for Cp*Co(III)-mediated regioselective [4 + 2]-annulation of **1** (Bond lengths in Å)

ortho-Cobaltation of $CoCp^*(OAc)_2$ via acetate-aided N-H, C−H deprotonation

With $CoCp^*(OAc)_2$ **A** in hand, the reaction between **1** and **A** denoted as path A is initiated from **i1** via **ts-i12** in step 1 with the activation energy barrier of 26.1 kcal mol^{-1} (Figure S2). The transition vector corresponds to the H1 transfer from N of **1** to O1 of one OAc ligand (1.08, 1.53 Å). N-H deprotonation is

aided by acetate exothermic by 15.4 kcal mol^{-1} in resultant **i2**, from which the nitrocobaltization takes place via **ts-i23** forming N-Co bond (1.96 Å) in stable complex **i3** in step 2 with activation energy of 21.3 kcal mol^{-1}. The transition vector of **ts-i23** contains the closing of N to Co simultaneously with the departure of O2 from Co (2.06, 2.31 Å). Although the OAc ligand no longer coordinates with Co after protonation, there is still O1H1···O3 H bond (1.60 Å). FMO calculations were applied for typical TSs to get more qualitative evidence of structural analysis.[26-30] The visual orbitals of Highest Occupied Molecular Orbital (HOMO) and Lowest Unoccupied Molecular Orbital (LUMO) were analyzed (Figure S4) together with MBO results for the orbital contribution of bonding atoms (Table 2). HOMO of **ts-i23** is located mainly on p orbital of N, d orbital of Co and minor on the lone pair electrons of O2. This distribution favors the concert coordinated N and uncoordinated O2 to Co, respectively. What's more, MBO values of N···Co, Co···O2 (0.518, 0.264) echoes the formation of N–Co bond, cleavage of Co–O2.

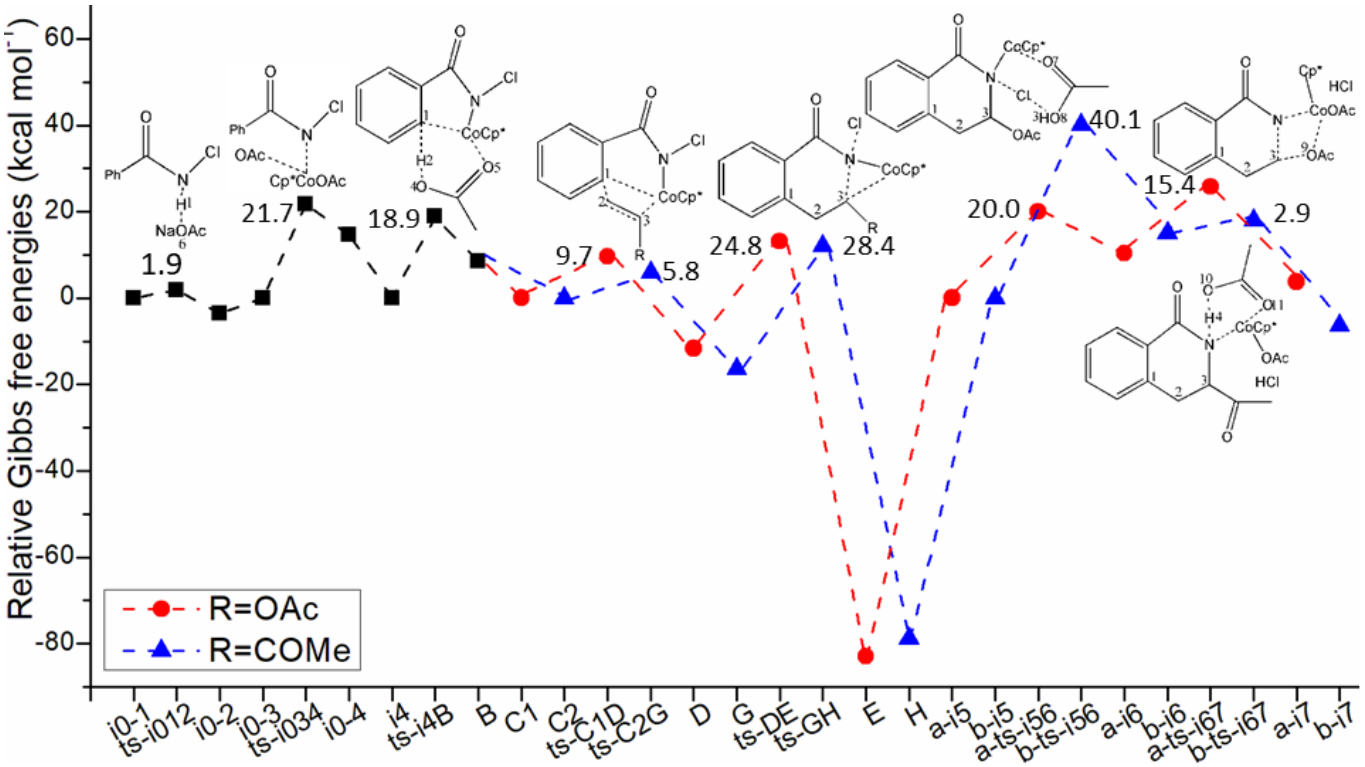

Figure 2. Relative Gibbs free energy profile in solvent phase starting from complex **i0-1**, **i0-3**, **i4**, **C** and **i5**

Table 2. Mayer bond order (MBO) of typical TSs

	N···Co	Co···O2		
ts-i23	0.518	0.264		
	C1···H2	H2···O4	C1···Co	Co···O5
ts-i4B	0.386	0.306	0.548	0.520
	C1···Co	C1···C2	C2···C3	C3···Co

ts-C1D	0.575	0.442	1.100	0.669
	C3⋯Co	C3⋯N	N⋯Cl	N⋯Co
ts-DE	0.431	0.379	0.256	1.132
	C3⋯O9	O9⋯Co	C3⋯N	N⋯Co
a-ts-i67	0.341	0.404	1.281	0.569
	O10⋯H4	H4⋯N	C3⋯N	N⋯Co
b-ts-i67	0.370	0.333	0.867	0.479

An alternative path is located considering NaOAc can also function as base to realize N-H deprotonation of **1**. As the starting point of relative Gibbs free energy profile (Figure 2), the energy of **i0-1** binding **1** and NaOAc is set as 0.0 kcal mol^{-1}, from which the proton shifts in step 1 via **ts-i012**, the transition vector of which is about the departure of H1 from N to O6 (1.27, 1.23 Å). This step not only involves a rather small activation energy barrier of only 1.9 kcal mol^{-1} but exothermic by -3.6 kcal mol^{-1}. Thus this path seems to be more favorable than previous one from step 1. The resultant **i0-2** is stable owing to the separated Na^+ and Cl^- not bonding to OAc of N (2.19, 1.81 Å). The optimized structure between deprotonated **1** and **A** is **i0-3** as the initial complex of step 2. This nitrocobaltization forming N-Co bond via **ts-i034** of path B is similar with that of path A via **ts-i23** both from the transition vector and activation energy. Therefore the path with NaOAc is preferred for N-H deprotonation process.

Once OAc is released, **i0-4** turns to be intermediate **i4**, which is taken as the starting point of step 3, namely the *ortho*-cobaltation via acetate-aided C−H deprotonation of the second OAc ligand. This step proceeds via **ts-i4B** with activation energy barrier of 18.9 kcal mol^{-1} endothermic by 8.5 kcal mol^{-1} furnishing a five-membered intermediate **B** with C1-Co bond (1.95 Å) and weakened coordination of HOAc to Co (2.03 Å). The transition vector of **ts-i4B** indicates the simultaneous bonding of C1-Co, leaving of H2 from C1 to O4 and cooperated away from O5 to Co (1.95, 1.33, 1.29 and 2.11 Å) (Figure S3a). The correctness of **ts-i4B** is also verified by FMO analysis. HOMO on bonding orbital of C1-H2, d orbital of Co and lone pair of O4, O5 facilitate the H2 capture of C1 by O4 and ring closing via C1-Co. This outcome echoes MBO values of C1⋯H2, H2⋯O4, C1⋯Co and Co⋯O5 (0.386, 0.306, 0.548, 0.520).

Coordinative insertion and reductive elimination/oxidative addition of CoCp*(I) species

Two kinds of alkene **2**a/**2**b are investigated subsequently. On the basis of same process, the reaction with **2**a (R=OAc) will be discussed in detail (red dash line of Figure 2). As the starting point binding **2**a and **B** without HOAc, the intermediate **C1** is a stable complex featuring π-coordination of alkene to Co with short C2⋯Co, C3⋯Co distances (2.21, 2.41 Å). **2**a undergoes coordinative insertion into C1-Co via

ts-C1D in step 1 with the activation energy barrier of 9.7 kcal mol^{-1} exothermic by -11.7 kcal mol^{-1}. The transition vector contains remarkable bonding of C1–C2 (1.99 Å), C3–Co (2.00 Å) and breaking of C1-Co (2.06 Å), stretching of C2–C3 double bond to single (1.43 Å) (Figure S3b). HOMO of **ts-C1D** is composed of bonding orbital of C1-C2 and anti-bonding orbital of C1-Co. MBO values of C1⋯Co, C1⋯C2 (0.575, 0.442) agrees well with this distribution.

Characterized by N-Co and C3-Co coordinated bond (2.0, 1.95 Å), the seven-membered cobaltacycle is afforded in resulting intermediate **D**, which transformed to six-membered intermediate **E** in step 2 via **ts-DE** with the activation energy barrier of 24.8 kcal mol^{-1} continuously release energy large to be -83.0 kcal mol^{-1}. The transition vector is about the closing of C3 to N and departure of C3–Co, N-Cl bond (2.14, 2.21, 2.47 Å) (Figure S3c). N-Co is still bonded to be 1.64 Å. HOMO of **ts-DE** distributed on bonding orbital of C3-N and anti-bonding orbital of N-Cl. This location is consistent with MBO values of C3⋯Co, C3⋯N, N⋯Cl (0.431, 0.379, 0.256). Function as an internal oxidant, the reductive elimination and oxidative addition of CoCp*(I) species result in N−Cl bond cleavage and new coordination of Cl to Co. Kinetically, step 1 is fairly easy. The step 2 is also favorable in thermodynamics with tremendous exothermic energy. Moreover, from the energy level of **ts-i4B** and **ts-DE** (18.9 and 13.1 kcal mol^{-1}), this is not conflict with the rate-limiting C-H insertion via **ts-i4B** proposed by Jeganmohan (Table 1). The outcome of reaction with **2**b (R=COMe) involves similar trend for two steps (blue dash line of Figure 2).

AcOH-assisted CoCp*$(OAc)_2$ recovery

The recovery of CoCp*(III) assisted by AcOH is different between the reaction with **2**a and **2**b. As the starting point of relative Gibbs free energy profile, the intermediate **a-i5** is a complex with weak coordinated relation of binding AcOH carbonyl and Co. Cl is protonated by AcOH hydroxyl in step 1 via **a-ts-i56** with activation energy barrier of 20.0 kcal mol^{-1} achieving the simultaneous dissociation of Co-Cl bond. The transition vector contains further closing of O7 to Co and H3 leaving from O8 to Cl (1.89, 1.55, 1.36 Å) (Figure S3d). Thus, newly formed OAc completely becomes one ligand of Co together with HCl molecule in the resultant **a-i6**, from which the barrier of step 2 is decreased to be 15.4 kcal mol^{-1} via **a-ts-i67**. Here, the breaking of OAc from the six-membered ring and binding to Co makes it the second acetate ligand provided by vinyl acetate **2**a. Meanwhile, N is uncoordinated to Co and C3-N is contracted from single to double. This concerted process is well indicated by the the transition vector of **a-ts-i67**. That is the leaving of O9 from C3 to Co and cleavage of N–Co, shortening of C3-N bond (1.94, 2.08, 1.97, 1.34 Å) (Figure S3e). The intermediate **F** is generated from the last stable complex **a-i7** with isolated recovered **A**. Finally, with OAc as the proton transfer station, two steps are needed for the basic

acetate-assisted tautomerization of **F** affording product **3**a. Both are pretty easy with small barriers lower than 10 kcal mol^{-1}.

When it comes to vinyl ketone **2**b with COMe group unable to coordinate with Co, two molecules of AcOH are required for **H** to realize the recovery of **A** and production of **3**b with COMe still bonded to ring. The step 1 is also the protonation of Cl by one AcOH via **b-ts-i56**. However, the barrier is increased to be 40.1 kcal mol^{-1} owing to the inconspicuous closing of O7 to Co, and H3 still bonded to O8 away from Cl (2.09, 1.05, 2.08 Å) compared with that of **a-ts-i56**. This not only approves **3**a and **3**b kinetic controlled products but echoes the higher yield of **3**a than **3**b in experiment (81%, 50%). Once HCl is formed, one OAc ligand is available for Co in **b-i6**, which contains strong H-bond between the second AcOH and N (1.63 Å) ready for the protonation of N next. The barrier of step 2 is rather small to be only 2.9 kcal mol^{-1} via **b-ts-i67**, of which the transition vector involves H4 leaving from O10 to N and simultaneous departure of N–Co (1.15, 1.38, 2.09Å) (Figure S3f). Hence another acetate ligand is supplied by the second AcOH in last **b-i7** assembled by recovered **A** and final intermediate **I**, the dehydrooxidation of which gives **3**b. The formation of HCl in rate-limiting step 1 coinciding for **2**a and **2**b helps the reconstruction of catalyst.

In view of the solvent effect on reaction with ions estimated by our approach,[26-30] the impact of solution is expected to be not obvious, just as the difference value of absolute energies between in gas phase and DCE solution listed for all stationary points (Table S1). Thankfully, the activation energies of most steps in solution phase are decreased compared with those in gas (Table S2). Accordingly, the promotion by Cp*Co(III) produced the most favorable influence of solvation on this regioselective [4 + 2]-annulation of *N*-chlorobenzamide with vinyl acetate or ketone from a kinetic point of view.

CONCLUSIONS

Our DFT calculations provide the first theoretical investigation on regioselective [4 + 2]-annulation of *N*-chlorobenzamide with two kinds of alkenes catalyzed by Cp*Co(III). The ortho-cobaltation via acetate-aided N-H and C−H deprotonation catalyzed by $CoCp^*(OAc)_2$ furnishes a five-membered intermediate, which is coordinative inserted into alkene by giving seven-membered cobaltacycle. The reductive elimination and oxidative addition of CoCp*(I) species afford six-membered ring. The recovery of CoCp*(III) is assisted by one AcOH for vinyl acetate with OAc group available to cleavage as one ligand. The product isoquinolin-1(2*H*)-one is yielded by acetate-assisted tautomerization. Two OAc ligands are both supplied by AcOH for vinyl ketone with COMe group difficult to break. Another product 3-acetylisoquinolin-1(2*H*)-one is given by the dehydrooxidation.

The decreased absolute energies in DCE solution compared with in gas suggest a favorable solvation effect kinetically. The promotion of Cp*Co(III) lies in the barrier decrease of most steps especially N-H

and C−H deprotonation. AcOH functions in the protonation of Cl, N and as sources of acetate ligands for the recovery of CoCp*(III). These results are supported by Multiwfn analysis on FMO of specific TSs and MBO value of vital bonding, breaking.

EXPERIMENTAL

The geometry optimizations were performed at the B3LYP/BSI level with the Gaussian 09 package.[31,32] The mixed basis set of LanL2DZ for Co and 6-31G(d) for non-metal atoms[26-30] was denoted as BSI. Different singlet and multiplet states were clarified with B3LYP and ROB3LYP approaches including Becke's three-parameter hybrid functional combined with Lee−Yang−Parr correction for correlation.[33,34] The nature of each structure was verified by performing harmonic vibrational frequency calculations. Intrinsic reaction coordinate (IRC) calculations were examined to confirm the right connections among key transition-states and corresponding reactants and products. Harmonic frequency calculations were carried out at the B3LYP/BSI level to gain zero-point vibrational energy (ZPVE) and thermodynamic corrections at 298.15 K and 1 atm for each structure in dichloroethane (DCE). The solvation-corrected free energies were obtained at the B3LYP/6-311++G(d,p) (LanL2DZ for Co) level in DCE by using integral equation formalism polarizable continuum model (IEFPCM) in Truhlar's "density" solvation model[35-39] on the B3LYP/BSI-optimized geometries.

As an efficient method obtaining bond and lone pair of a molecule from modern ab initio wave functions, NBO procedure was performed with Natural bond orbital (NBO3.1) to characterize electronic properties and bonding orbital interactions.[40-42] The wave function analysis was provided using Multiwfn_3.7_dev package[43] including research on frontier molecular orbital (FMO) and Mayer bond order (MBO).

SUPPLEMENTARY DATA

Supplementary data [Computation information and cartesian coordinates of stationary points; Calculated relative energies for the ZPE-corrected Gibbs free energies (ΔGgas), and Gibbs free energies (ΔGsol) for all species in solution phase at 298 K; Optimized structures of selected intermediates and transition states.] associated with this article can be found, in the online version, at URL: https://www.heterocycles.jp/newlibrary/downloads/PDFsi/27977/106/8

ACKNOWLEDGEMENTS

This work was supported by National Natural Science Foundation of China (21973056, 21972079) and Natural Science Foundation of Shandong Province (ZR2019MB050).

REFERENCES AND NOTES

1. E. Kiselev, D. Sooryakumar, K. Agama, M. Cushman, and Y. Pommier, *J. Med. Chem.*, 2014, **57**, 1289.
2. Z. J. Song, D. M. Tellers, P. G. Dormer, D. Zewge, J. M. Janey, A. Nolting, D. Steinhuebel, S. Oliver, P. N. Devine, and D. M. Tschaen, *Org. Process Res. Dev.*, 2014, **18**, 423.
3. R. S. Phatake, P. Patel, and C. V. Ramana, *Org. Lett.*, 2016, **18**, 2828.
4. G.-D. Xu and Z.-Z. Huang, *Org. Lett.*, 2017, **19**, 6265.
5. J.-R. Huang and C. Bolm, *Angew. Chem. Int. Ed.*, 2017, **56**, 15921.
6. L. Song, Z. Lv, Y. Li, K. Zhang, E. V. Van der Eycken, and L. Cai, *Org. Lett.*, 2023, **25**, 2996.
7. A. Ghosh, G. T. Sapkal, and A. B. Pawar, *J. Org. Chem.*, 2023, **88**, 4704.
8. Z. Yang, J. Liu, Y. Li, J. Ding, L. Zheng, and Z.-Q. Liu, *J. Org. Chem.*, 2022, **87**, 14809.
9. Y. Zhu, R. Dai, C. Huang, W. Zhou, X. Zhang, K. Yang, H. Wen, W. Li, and J. Liu, *J. Org. Chem.*, 2022, **87**, 11722.
10. P. Ma, Y. Wang, J. Wang, and N. Ma, *J. Org. Chem.*, 2023, **88**, 7425.
11. F. Wang, S. Yu, and X. Li, *Chem. Soc. Rev.*, 2016, **45**, 6462.
12. D.-S. Kim, W.-J. Park, and C.-H. Jun, *Chem. Rev.*, 2017, **117**, 8977.
13. W. Ali, G. Prakash, and D. Maiti, *Chem. Sci.*, 2021, **12**, 2735.
14. X. Wang, J. Zhang, Y. He, D. Chen, C. Wang, F. Yang, W. Wang, Y. Ma, and M. Szostak, *Org. Lett.*, 2020, **22**, 5187.
15. S. Prakash, R. Kuppusamy, and C.-H. Cheng, *ChemCatChem*, 2018, **10**, 683.
16. N. Muniraj, A. Kumar, and K. R. Prabhu, *Adv. Synth. Catal.*, 2020, **362**, 152.
17. A. Dey and C. M. R. Volla, *Org. Lett.*, 2021, **23**, 5018.
18. A. Dey and C. M. R. Volla, *Org. Lett.*, 2020, **22**, 7480.
19. T. Rogge, J. C. A. Oliveira, R. Kuniyil, L. Hu, and L. Ackermann, *ACS Catal.*, 2020, **10**, 10551.
20. A. Nandy and H. J. Kulik, *ACS Catal.*, 2020, **10**, 15033.
21. R. Sun, X. Yang, Q. Li, K. Xu, J. Tang, X. Zheng, M. Yuan, H. Fu, R. Li, and H. Chen, *Org. Lett.*, 2019, **21**, 9425.
22. R. Mandal, B. Emayavaramban, and B. Sundararaju, *Org. Lett.*, 2018, **20**, 2835.
23. R. Mandal, B. Garai, and B. Sundararaju, *J. Org. Chem.*, 2021, **86**, 9407.
24. P. B. De, S. Atta, S. Pradhan, S. Banerjee, T. A. Shah, and T. Punniyamurthy, *J. Org. Chem.*, 2020, **85**, 4785.
25. S. J. Murugan and M. Jeganmohan, *J. Org. Chem.*, 2023, **88**, 1578.
26. H. Lv, F. Han, N. Wang, N. Lu, Z. Song, J. Zhang, and C. Miao, *Eur. J. Org. Chem.*, 2022, e202201222.

27. H. Zhuang, N. Lu, N. Ji, F. Han, and C. Miao, *Adv. Synth. Catal.*, 2021, **363**, 5461.
28. N. Lu, X. Lan, C. Miao, and P. Qian, *Int. J. Quantum Chem.*, 2020, **120**, e26340, https://doi.org/10.1002/qua.26340.
29. N. Lu, H. Liang, P. Qian, X. Lan, and C. Miao, *Int. J. Quantum Chem.*, 2020, **120**, e26574, https://doi.org/10.1002/qua.26574.
30. G. Frenking and N. Fröhlich, *Chem. Rev.*, 2000, **100**, 717.
31. M. J. Frisch, G. W. Trucks, H. B. Schlegel, G. E. Scuseria, M. A. Robb, J. R. Cheeseman, G. Scalmani, V. Barone, B. Mennucci, G. A. Petersson, H. Nakatsuji, M. Caricato, X. Li, H. P. Hratchian, A. F. Izmaylov, J. Bloino, G. Zheng, J. L. Sonnenberg, M. Hada, M. Ehara, K. Toyota, R. Fukuda, J. Hasegawa, M. Ishida, T. Nakajima, Y. Honda, O. Kitao, H. Nakai, T. Vreven, J. A. Montgomery Jr., J. E. Peralta, F. Ogliaro, M. Bearpark, J. J. Heyd, E. Brothers, K. N. Kudin, V. N. Staroverov, R. Kobayashi, J. Normand, K. Raghavachari, A. Rendell, J. C. Burant, S. S. Iyengar, J. Tomasi, M. Cossi, N. Rega, J. M. Millam, M. Klene, J. E. Knox, J. B. Cross, V. Bakken, C. Adamo, J. Jaramillo, R. Gomperts, R. E. Stratmann, O. Yazyev, A. J. Austin, R. Cammi, C. Pomelli, J. W. Ochterski, R. L. Martin, K. Morokuma, V. G. Zakrzewski, G. A. Voth, P. Salvador, J. J. Dannenberg, S. Dapprich, A. D. Daniels, Ö. Farkas, J. B. Foresman, J. V. Ortiz, J. Cioslowski and D. J. Fox, *Gaussian 09 Revision B.01*, Gaussian, Inc, Wallingford, CT 2009.
32. P. J. Hay and W. R. Wadt, *J. Chem. Phys.*, 1985, **82**, 270.
33. A. D. Becke, *J. Chem. Phys.*, 1996, **104**, 1040.
34. C. T. Lee, W. T. Yang, and R. G. Parr, *Phys. Rev. B*, 1988, **37**, 785.
35. O. Tapia, *J. Math. Chem.*, 1992, **10**, 139.
36. J. Tomasi and M. Persico, *Chem. Rev.*, 1994, **94**, 2027.
37. B. Y. Simkin and I. Sheikhet, Quantum Chemical and Statistical Theory of Solutions—A Computational Approach, Ellis Horwood, London, 1995.
38. J. Tomasi, B. Mennucci, and R. Cammi, *Chem. Rev.*, 2005, **105**, 2999.
39. A. V. Marenich, C. J. Cramer, and D. G. Truhlar, *J. Phys. Chem. B*, 2009, **113**, 6378.
40. A. E. Reed, R. B. Weinstock, and F. Weinhold, *J. Chem. Phys.*, 1985, **83**, 735.
41. A. E. Reed, L. A. Curtiss, and F. Weinhold, *Chem. Rev.*, 1988, **88**, 899.
42. J. B. Foresman and A. Frisch, Exploring Chemistry with Electronic Structure Methods, 2nd ed., Gaussian, Inc., Pittsburgh 1996.
43. T. Lu and F. Chen, *J. Comput. Chem.*, 2012, **33**, 580.